3.

Characterizing the Physical Oceanography of Coastal Waters Off Rhode Island, Part 2: New Observations of Water Properties, Currents, and Waves

Prepared for the Rhode Island Ocean Special Area Management Plan 2010

By

David S. Ullman and Daniel L. Codiga

University of Rhode Island, June 30, 2010

PARTIALLY COMPLETE DRAFT
NOT READY FOR DISTRIBUTION OR EXTERNAL REVIEW

Executive Summary

Part 2 of the Rhode Island Ocean Special Area Management Plan physical oceanography characterization study complemented the review of archival observations and model runs carried out in Part 1 by focusing on the collection and analysis of new observations that can help provide a more complete description of the seasonal mean and variability of the water column structure, circulation, and waves. The physical oceanography of Rhode Island coastal waters is investigated using a combination of wide-area vessel-based surveys of water properties at 3-month intervals and long-term moorings at 5 sites to collect observations of hydrography, waves, and currents. The results improve our understanding of the seasonal cycle in the OSAMP region and also demonstrate the marked inter-annual variability that is manifest in the region.

The surveys and moored observations of hydrography during the period from September 2009 to July 2010 generally agree with the hydrographic climatology analyzed in Part 1. However, during late autumn/early winter of 2009, the observational program observed a previously undocumented intrusion of warm salty water, normally found near the shelf break, into the OSAMP region. The properties of this water, which floods the deep areas of the region during December 2009, are far different from our best prior estimate of the mean regional properties.

Currents measured by moored instruments at four locations are broken in to tidal and subtidal components. Tidal currents are dominated by semidiurnal components and tidal current ellipses reflect geographic amplification associated with nearby estuaries, and vertical structure of frictional bottom boundary layer, in very good agreement with previous observations and modeling. Subtidal currents have energetic weather band variability, which is strongly shaped by wind variations and dominates the longer-term residual circulation.

Waves have typical significant heights of 2-4 m and typical dominant periods of several seconds, both tending toward the lower/higher end of these ranges in summer/winter. During storm events the significant wave height reaches up to 7m and the dominant wave period reaches 14 s. The direction of peak wave energy is most commonly northward and slightly eastward, and variability in the direction is more pronounced at offshore sites.

Table of Contents

List of Figures

List of Tables

Abstract

(PREPARATION UNDERWAY)

1 Purpose and Scope

The purpose of this report, which is Part 2 in a two-part series and complements the review of previously gathered information in Part 1 (Codiga and Ullman 2010), is to present new observations collected to characterize water properties, currents, and waves in the Rhode Island Special Area Management Plan (OSAMP) region. These observations expand on prior investigations through use of modern measurement techniques and by exploring geographic areas that have, as described in Part 1, received almost no previous attention. For water properties, the emphasis is on geographic and vertical structure, and seasonal changes. For currents, the emphasis is on descriptions of tidal fluctuations, weather-band variability (changes on timescales of about 1 to 10 days), and longer-term means at four specific locations, including comparisons among the sites. Surface wave parameters from five locations are described. The reader is referred to Part 1 for overall context, including descriptions of the geographic and bathymetric setting (see Figures 1 and 2 of Codiga and Ullman 2010).

In addition to temperature and salinity, the water properties analysis includes measurements of dissolved oxygen, Chlorophyll fluorescence, photosynthetically active radiation, and turbidity; while the latter four quantities are described briefly here, for more complete discussion of their implications to biological and sediment transport processes the relevant companion OSAMP reports should be consulted. Similarly, while our analysis presents wind measurements, it does so solely for context in interpreting currents; for a comprehensive description of winds reference should be made to the dedicated OSAMP report. Tidal and weather-band fluctuations in sea level are addressed here but the durations of the observations do not permit us to address climatic change in sea level, which is taken up in a separate OSAMP report. Finally, the treatment of wave observations here is cursory because a companion OSAMP report includes a thorough investigation of wave processes based on both these observations and an intensive modeling effort.

2 Introduction

Temperature and salinity characteristics across sizable portions of the OSAMP domain, particularly eastern Rhode Island Sound (RIS), are historically severely under-sampled. This was made clear by the review of available temperature and salinity observations in Part 1, and was a primary motivation for the seasonal series of vessel-based conductivity-temperature-depth (CTD) surveys completed and described here. In order to capture vertical structure and

geographic patterns, the surveys include profiles spanning the water column at stations covering the entire OSAMP domain with nominal spacing of 8-12 km (Figure 1). The station grid is nearly identical to that used in Part 1 for explorations of historical observations and model outputs, so facilitates direct comparisons. The goal of the surveys was to characterize the seasonal cycle, so one 2-3 day survey was completed in each of September 2009, December 2009, March 2010, and June 2010. In addition to temperature and salinity the surveys measured water properties relevant to biological and sediment transport processes (straightforward using modern instrumentation): dissolved oxygen, Chlorophyll fluorescence, photosynthetically active radiation, and turbidity. The maps and sections of these quantities presented here are a considerable advance over previously available observations of them.

A series of deployments of moored instrumentation captured temporal variability of temperature, salinity, currents and waves on timescales from hours to seasons in order to complement the broad geographic coverage but minimal temporal resolution and of the vessel-based water property surveys. Moored instruments sampled a total of five sites (Figure 2, Table 1).

At two sites, moorings instrumented with a suite of water-column sensors (temperature, salinity, currents), accelerometers to measure wave properties, and meteorological sensors (winds, temperature, pressure) were maintained continuously year-round starting in October 2009. The deployments were carried out by University of Maine under subcontract, as part of the Northeastern Regional Association of Coastal Ocean Observing Systems (NERACOOS), and data was delivered and distributed in real time. These two moorings are denoted MD-S and MD-F; MD indicates Multi-Disciplinary (both meteorological and physical oceanographic parameters were sampled), S indicates the site is in RI state waters south of Block Island, and F indicates the site is in federal waters in southeastern Rhode Island Sound.

To provide improved understanding of geographic variations in water column properties (temperature, salinity, and currents) and wave attributes, moored instruments were deployed at two additional sites that complement MD-S and MD-F. One was located about 10 km SE of MD-S, to help characterize the transition toward deeper water, and the second was located about 15 km NNW of MD-F, to help understand how properties change inshore of MDF towards central RIS. At these complementary sites, only physical oceanographic parameters were sampled, hence they are referred to a PO-S and PO-F respectively. Note that, despite its name, the PO-S site is not in state waters. The PO-S and PO-F moorings were maintained for two deployments,

one in late Fall 2009 (denoted FA09) and one in late Spring 2010 (denoted SP10), as year-round sampling was not possible given budgetary and logistical constraints. As these instruments were not intended for real time sampling they recorded and stored data internally.

At a fifth site the Army Corps of Engineers established a Datawell directional wave buoy, denoted the Block Island Wave Buoy (BIWB) although it is located offshore from central RIS. It has operated continuously since October 2009 and its real-time data stream is managed by the Coastal Data Information Program (CDIP) at Scripps Institution of Oceanography.

3 Methods

3.1 Vessel-Based Water Properties Surveys

Four vessel-based surveys, at approximately 3-month intervals covering the seasonal cycle, were carried out from the University of Rhode Island's research vessel Hope Hudner. The station grid (Figure 1) extends across eastern Block Island Sound (BIS), Rhode Island Sound (RIS), and the offshore area to the south. Surveys took 2-3 days to complete (see Table 2 for the survey dates) and were made without regard to tidal phase. During the December 2009 survey, not all stations were occupied (the omitted stations are obvious in the maps presented below) due to weather conditions.

At each station, vertical profiles of electrical conductivity (C), temperature (T), pressure (P), oxygen concentration (O_2), chlorophyll fluorescence, turbidity, and photosynthetic active radiation (PAR) were obtained using a hand-lowered package. The sensors included a SeaBird Electronics SBE 19plus CTD, with T, C, and O_2 (SBE 43) sensors located within a pumped duct; a Turner Designs SCUFA 2000-007 Fluorometer; and a BioSpherical QSP2300 PAR sensor.

The data were processed using SeaBird's data processing software (SBE Data Processing), including corrections for sensor alignment, conductivity cell thermal mass, and the response time of the O_2 sensor. Salinity was computed from the measured C, T, and P data, and all variables were averaged into 1 dbar (~1m) vertical bins. Chlorophyll fluorescence measurements were converted to chlorophyll concentrations using a generic calibration. The vertical profiles of PAR were used to estimate the light extinction coefficient by fitting the observed data to an exponential function: $I(z) = I_0 e^{-kz}$, where *I(z)* is light intensity at depth z, I_0 is the intensity at the surface (z=0), and k is the extinction coefficient (units m^{-1}). For profiles where the CTD was not shaded by the survey vessel at the surface, the fits were performed using observations from the surface down to a depth at which the sensor response was observed to roll off. When the CTD

was shaded at the surface, the upper 5-10 m of the profile was omitted from the fit. The depth of the euphotic zone was estimated as the depth at which the light intensity was 1% of the surface value (I_0).

3.2 MD-S and MD-F Moored Instrumentation

On the MD-S and MD-F moorings the subsurface instrumentation (Table 1) included three CTDs, a 2m-deep Aanderaa 3429 current/temperature sensor recording once per hour, and a downward-looking Teledyne RD Instruments 600 kHz acoustic Doppler current profiler (ADCP) that sampled each meter from 5 m deep to within 3-4 m of the seafloor using 6-second ping interval for 8 minutes once an hour. The CTDs were SeaBird Electronics 37 Series; one mounted on the buoy sampling each 30 minutes, one on the mooring wire in the upper water column, and one on the wire nearest the seafloor, the latter two sampling each 60 minutes and sending their data inductively to a coupler at the top of the wire rope. Wave parameters were measured by a Summit 34103A accelerometer package on the buoy operating at 2 Hz for a 17-minute interval each 30 minutes. The meteorological package included redundant Gill WindSonic wind sensors at 4m above sea level, and a Campbell 107L temperature sensor and Setra 270 barometric pressure sensor both at 3m above sea level.

3.3 PO-S and PO-F Moored Instrumentation

During each period (FA09 and SP10), a mooring instrumented with 7 CTD sensors distributed through the water column, and an upward-looking acoustic Doppler current profiler (ADCP) in a bottom frame very close nearby, were both deployed. The CTDs, measuring pressure as well as temperature and conductivity, consisted of a Falmouth Scientific Instruments NXIC bracketed to the buoy, sampling at 6 Hz for about 10 seconds each 90 seconds, and six SBE-37SM Microcats on the wire rope below sampling once each 16 seconds. After passing the data through a 3 point running median filter to remove spurious values, the CTD data were averaged into 4-minute ensembles.

The ADCP was a Teledyne RD Instruments 600 kHz deployed and recovered in a Mooring Systems Incorporated bottom frame. It measured currents each meter from about 2-3 m off the seafloor to about 3-4 m below the surface, with pings each 6 seconds and 20-minute ensemble averaging interval. The ADCP also measured wave orbital motions and computed directional wave parameters, using a 20-minute burst of 1 Hz sampling each 2 hours.

3.4 BIWB Moored Instrumentation

The BIWB is a Datawell directional buoy measuring significant wave height, peak wave period, and peak wave direction, based on 17-minute bursts of sampling each 30 minutes. Details of the processing are provided at the CDIP website, cdip.ucsd.edu.

3.5 Analysis techniques

Tidal analysis was carried out using the t-tide software package (Pawlowicz et al. 2002). Sub-tidal quantities were calculated using a 25-hour halfwidth triangle-weight low-pass filter and subsampled to 12-hourly values.

4 Water Properties

4.1 Maps & Sections of Hydrographic Parameters from Vessel-Based Surveys

We present the observations in two forms: (1) maps showing variables at a given depth below the water surface or height above the bottom, and (2) vertical sections along the approximately north-south and east-west lines shown in Figure 1. Although the data are treated as if the stations were sampled synoptically, it should be borne in mind that 2-3 days were required to complete the surveys. Therefore some smearing of features is expected due to advection of features by tidal and subtidal currents as well as by temporal evolution of the fields. Should note the times of spring and neap tides relative to the survey dates.

4.1.1 Temperature

During the late summer hydrographic survey in September 2009 (Figure 3, Figure 4, Figure 6), near-surface temperature gradients are generally small. This is in contrast to the observation, in satellite-derived sea surface temperature (SST) climatologies (e.g. Codiga and Ullman, 2010), of a moderately strong temperature front ($\Delta T \sim$ 1-2 °C) separating cooler BIS waters from warmer RIS and offshore waters. Strong near-bottom gradients occur along the 40 m isobath on the south side of Coxes Ledge (southern end of lines NS6 and NS7) and between the 30 m and 40 m isobaths south of Block Island. A deep thermocline (~30 m or deeper) is observed in central RIS and in the areas offshore of RIS and BIS, whereas in BIS and north-central RIS there is little vertical temperature structure. Vertical temperature differences range from less than 1.5 °C along the northern edge of the survey region to around 7 °C in the offshore region south of RIS. At the offshore end of line NS7, a thin layer of warm (18-19 °C) water is observed just above the thermocline (~30 m depth). Examination of the corresponding salinity section (Figure

9) shows that this water is saltier than the water above and below, suggesting that this feature is an intrusion of outer shelf water similar to those observed in earlier surveys.

Whereas the late summer survey observed warmer surface water temperatures than deep temperatures, during the early winter survey in December 2009 (Figure 3, Figure 4, Figure 6), the temperature gradient is reversed with coolest water near the surface and warmest water at depth. Vertical temperature differences range from near zero in BIS and the shallower northern and eastern parts of RIS to 4-5 °C at the offshore end of line NS3 south of Block Island. Near-surface temperatures generally decrease towards the north and east where the shallow water column tends to cool most rapidly in late fall. However, as during summer, near-surface temperature gradients are weaker than those at depth. Near the bottom, highest gradients occur in the region south of Block Island and in central RIS associated with the edges of a warm patch centered on the deep channel extending northeast into central RIS. Water temperatures at depth in this patch, which appears to be contiguous with offshore deep waters south of Block Island , are greater than 15 °C. Temperatures in this region are anomalously high compared to temperatures during fall (≤13 °C) and winter (≤6 °C) at the seafloor in the climatology and the model output examined by Codiga and Ullman (2010). As will be discussed in the next section, this water is also anomalously salty, suggesting outer shelf origin.

During the late winter survey in March 2010 (Figure 3, Figure 5, Figure 7), the range of observed temperature over the whole region is quite small (range of 2-4 °C over the entire region at all depths) reflecting the homogenization of temperature due to strong surface cooling in winter (and possibly the offshore retreat of the anomalously warm deep water observed in late autumn). Coldest water during this survey was located near the bottom in northeast RIS while warmest temperatures were observed near the surface in the western half of the survey region. The relatively warm surface layer in BIS and western RIS was less than 10 m thick.

The late spring hydrographic survey in June 2010 (Figure 3, Figure 5, Figure 7) shows the re-emergence of strong thermal stratification in the region. Vertical surface to bottom temperature differences range from 2-3 °C in BIS and northeastern RIS to ~10 °C at the offshore edge of the survey region. Surface temperatures in BIS are ~2 °C cooler than surface waters offshore and in RIS, consistent with the SST climatology of Codiga and Ullman (2010). As was seen in the September survey, large gradients in near-bottom temperature occur, but during this survey the high-gradient region is shifted to shallower areas (roughly the 30 m isobath). This shift is probably explained by the shallower temperature surface mixed layer during the June survey

compared to September. In this interpretation, the high near-bottom gradients are found where the thermocline intersects the bottom.

4.1.2 Salinity

The salinity field during the September 2009 survey (Figure 8, Figure 9, Figure 11) is dominated by the low-salinity outflow from LIS. Near surface salinities increase from less than 31 psu in central/western BIS to greater than 31.5 psu in central RIS to greater than 32 psu in offshore areas. Near-bottom salinities increase by roughly the same amount (~1.5 psu) over the same areas with some indication that the horizontal gradient steepens in the southwest corner of the survey region where the coastal current associated with the LIS outflow onto the continental shelf is known to lie (Ullman and Codiga, 2004). Vertical salinity stratification is strongest in BIS where surface to bottom differences of up to 2 psu occur, and weakest to the east and offshore (except for the westernmost portion of the offshore zone which is influenced by the aforementioned coastal outflow). Although salinity generally increases with depth (and distance eastward), the highest salinities in the entire region occur in the thin intrusive feature identified in the temperature data (see section 4.1.1) at about 30 m depth at the offshore end of line NS7. The maximum observed salinity in this intrusion (which is also warmer than water above and below) is approximately 33.5 psu, which according to the shelfbreak front climatology of Linder and Gawarkiewicz (1998) is outer shelf water found on average on the inshore side of the shelfbreak front.

In the December survey (Figure 8, Figure 9, Figure 11), observed near-bottom salinities in areas of the survey region with water depth greater than about 35 m are extremely high. Salinity in the deep channel north and west of Coxes Ledge is greater than 34 psu and the peak salinity of greater than 34.5 is observed at the offshore end of line NS3. Note that the offshore station of line NS4 was not sampled during this survey and it is possible that the high salinity core is larger than it appears in Figure 8. Nonetheless, the deep water observed in the December survey is clearly anomalous (compare with peak near-bottom salinities of 33.25 psu in the fall and winter SAMP region climatology (Codiga and Ullman, 2010)). In fact the shelfbreak front climatology of Linder and Gawarkiewicz (1998) puts the 34.5 isohaline in the center of the front, intersecting the bottom on average at approximately the 100 m isobath. Minimum surface salinity of less than 31 psu was observed in the December 2009 survey in west/central BIS. This value is approximately the same as the minimum value observed in the September survey, although the areal extent of the low salinity region appears to be somewhat reduced. Examination of the

SAMP climatological surface salinity in west/central BIS, shows that the observed December values are approximately equal to the fall climatological values and are fresher (by several tenths of a psu) than the winter means.

Strongest near-surface horizontal salinity gradients in the December survey are observed on the shelf southwest of Block Island (as in September) and also in northeastern RIS. In northeast RIS, on lines NS7 and NS8, a surface-layer front with cross-frontal salinity difference of approximately 0.5 psu over 10 km is observed (Figure 9). The front weakens slightly in the RIS sections to the west (NS4 – NS6) and appears to become more surface-trapped there. Vertical surface-bottom salinity differences during the December survey ranges from several tenths of a psu in BIS to ~ 3 psu in the offshore regions influenced by the high salinity intrusion discussed above.

The March 2010 survey found the deep salinity in the deep central RIS and offshore regions to be greatly reduced from the December values (Figure 8, Figure 10, Figure 12) indicating offshore retreat of the presumed outer shelf water (or alongshore advection out of the OSAMP survey region). Maximum salinity during the March survey was ~32.5 psu, while the freshest water, at the surface in west/central BIS, was less than 29.5 psu. Near-surface salinities increase rapidly towards eastern BIS and the front between the freshest water and RIS and shelf surface water extends from eastern BIS southwest onto the shelf to the southwest of Block Island. The sloping front on the shelf south of BIS intersects the bottom roughly between the 30 m and 40 m isobaths. Vertical salinity stratification in BIS is much stronger during March 2010 than during the previous surveys, with surface-bottom salinity differences of ~2 psu there. Salinity stratification weakens towards the east, with surface-bottom differences of less than 1 psu in eastern RIS. However, even in eastern RIS, there is evidence of a slightly freshened (S ~ 31 psu) lens of relatively low salinity water at the northern edge of the survey region.

During the June 2010 survey period (Figure 8, Figure 10, Figure 12), the observed salinity range is slightly reduced from that encountered in the March survey. Minimum observed salinity in west/central BIS was about 0.5 psu saltier (~30 psu), while maximum salinity at depth offshore is approximately the same (32-32.5 psu). Eastern BIS and central RIS are fresher (by ~0.5 psu) in June as compared with March, suggesting an expansion of the region influenced by the outflow from LIS. Horizontal as well as vertical gradients of salinity are somewhat reduced in June compared to March. There is a weak signal of freshening along the edge of the survey region in northeast RIS.

4.1.3 Dissolved Oxygen

Dissolved oxygen levels during the September 2009 survey (Figure 13, Figure 14, Figure 16) generally decrease with depth. The near surface concentration in west/central BIS is in the range 7-8 mg/l and increases towards the east, reaching 8-9 mg/l in surface waters of eastern RIS. Near-bottom oxygen concentration is generally 6-7 mg/l except for a portion of north/central RIS (northern part of lines NS5 and NS6) where concentrations fall to around 5 mg/l.

In December oxygen concentrations in the bottom water of north/central RIS are increased above the levels observed in September (Figure 13, Figure 14, Figure 16). Concentrations during December are above 6 mg/l. Lowest concentrations during the December survey occur near the bottom in the deep channel of central RIS, the area of apparent deep intrusion of outer shelf water. Surface oxygen levels in December are everywhere above 8 mg/l. During the March 2010 survey when water temperatures are at a minimum, oxygen concentrations are uniformly high throughout the water column with values above 10 mg/l everywhere (Figure 13, Figure 15, Figure 17).

The June 2010 survey found dissolved oxygen concentrations (Figure 13, Figure 15, Figure 17) reduced significantly over the March values, presumably in part due to the increase in water temperatures. The region of low concentration in north/central RIS appears to be redeveloping, with concentrations of 6-7 mg/l observed at the north end of line NS5. A significant feature during the June survey is a subsurface oxygen maximum with concentrations above 9 mg/l occurring in bands of order 10 m thick in the southern, offshore region of the survey. The location of the most intense of these maxima is typically at depths of 20-30 m, although there are places where the maximum is found at depths of 10-20 m. As will be discussed in Section 4.1.4, subsurface maxima in Chlorophyll concentration were detected in the June survey and it is likely that the oxygen maxima observed here are a result of phytoplankton photosynthesis.

4.1.4 Chlorophyll

Near-surface chlorophyll concentrations (derived from fluorometric measurements) during the September 2009 survey are below 4 μg/l throughout the survey region (Figure 18, Figure 19, Figure 21). Highest values occur around Block Island and lowest concentrations (less than 1 μg/l) are found in the southern and eastern portions of the survey region. The vertical sections (Figure 19, Figure 21) show that chlorophyll concentrations are often elevated at mid-water depths. These subsurface maxima, with concentrations reaching ~10 μg/l in places but usually 5-

6 μg/l, are detected at various depths, ranging from near the bottom on lines NS8 and NS9 to approximately 10 m depth along lines NS1 – NS3. In general, phytoplankton biomass as measured by chlorophyll concentration tends to be highest in northwestern RIS and BIS and also in eastern RIS.

Chlorophyll levels in December 2009 (Figure 18, Figure 19, Figure 21) are somewhat lower than were found during the September survey. Near-surface levels are below 3 μg/l, but the region of highest concentration has shifted to central and eastern RIS. In most parts of the survey region, chlorophyll is low throughout the water column in December, although a weak subsurface maximum (3-4 μg/l) was detected at several stations in central RIS.

In March 2010, very low chlorophyll concentrations were observed throughout the OSAMP survey region (Figure 18, Figure 20, Figure 22). Surface values are less than 1 μg/l, and concentrations at depth are generally lower than 2 μg/l, except in northeast RIS. In that region, near bottom chlorophyll levels of 3-4 μg/l are observed.

Surface chlorophyll concentrations during the June 2010 survey (Figure 18, Figure 20, Figure 22) remained at low levels, less than 1 μg/l over most of the region and only 1-2 μg/l around Block Island and in isolated areas along the northern and western periphery of the survey region. In much of the region, especially central and southern RIS and BIS, a subsurface chlorophyll maximum was observed, with concentrations of up to approximately 5 μg/l at depths of 20-30 m.

4.1.5 Turbidity

Estimates of water turbidity from the fluorometer were below 1 nephelometric turbidity units (NTU) during the September 2009 survey (Figure 23, Figure 24, Figure 26). Highest values (0.75-1.0 NTU) were detected in BIS and near the bottom in the shallowest areas along the northern edge of the survey region. Values in the middle of the water column in central RIS are lower (~0.5 NTU). High near surface turbidity approaching 1 NTU was detected at station 47 near the offshore end of line NS7. Adjacent stations did not exhibit a similar elevation suggesting either an instrument malfunction or the presence of a very small scale feature. The lack of a corresponding signal in either the Chlorophyll concentration (Figure 19) or the depth of the euphotic zone (Figure 28, to be discussed in Section 4.1.6) suggests the former explanation.

Turbidity values during the December 2009 survey (Figure 23, Figure 24, Figure 26) appear to have been significantly higher than during September. Highest values (1.25-1.5 NTU) were

detected in northeastern RIS. Moderately high turbidity (0.75-1.0 NTU) was observed in west/central BIS with decreasing turbidity towards the east.

During the March 2010 survey, turbidity was low throughout the survey region, with values below 0.75 NTU everywhere (Figure 23, Figure 25, Figure 27). Highest turbidity (above 0.5 NTU) was detected in northern RIS and in BIS, with offshore values generally low.

Near-surface turbidity in June 2010 was generally very low, with values in the range of 0.25 – 0.5 NTU (Figure 23, Figure 25, Figure 27). Near bottom turbidity was elevated to 0.5-0.75 NTU in west/central BIS and in the far northeast corner of the survey region.

4.1.6 Euphotic Zone Depth

The estimated depth of the euphotic zone during the September survey was quite variable, ranging from ~10 m to 40 m (Figure 28). Highest values occur in central RIS and in the offshore areas and lowest values in BIS and in the far eastern portion of the survey region. The boundary between the BIS region of shallow euphotic zone depth and the region of deeper light penetration to the south and east is quite sharp and extends continuously from Pt. Judith southwest past Block Island to the southwest corner of the survey region. During the December survey, the euphotic zone depth is generally less than 20 m, with a general increase in the offshore direction, although without the sharp frontal boundary observed in September. In March 2010, the depth of the euphotic zone is everywhere greater than 20 m with some increase offshore. During June, the map of the euphotic zone depth resembles the September map, with low values (less than 20 m) in BIS and around the periphery of RIS and higher values offshore (30-40 m).

4.2 Temperature and Salinity Time Series from Moored Instruments

4.2.1 Fall 2009 Deployment

The PO-F and PO-S CTD moorings were deployed in mid-September 2009 with planned recovery in mid-December 2009. However, adverse weather conditions prevented us from carrying out this operation until mid January (see Table 1 for details on the mooring deployments). The Microcats filled their onboard memory in late December (28 Dec., 17:00 UTC) and no data were recorded after this time. Upon recovery (at a location 1 km to the southwest of its deployment location), the PO-S CTD mooring showed clear signs that it had been dragged by a trawler. Two instruments (nominally at depths of 12 and 20 m) were severely damaged and no data were recovered. Other instruments, although damaged, provided useful data for various lengths of time. One instrument (nominally at a depth of 7 m) was moved on the

mooring wire to a final depth of ~3 m below the surface. The lengths of the data records from the various instruments can be deduced from the instrument pressure records shown in Figure 29.

The pressure records from the CTDs at moorings PO-F and PO-S (Figure 29) provide information on the vertical motion of the instruments in response to waves and currents. The instruments are seen to experience correlated upward excursions of up to 2-3 m on time scales of days. The magnitude of the depth excursions appears to increase with the nominal depth of the instruments. In the analysis that follows, no attempt has been made to correct for the vertical motion of the sensors. The CTDs on moorings MD-F and MD-S were not equipped with pressure sensors, so no such analysis could be performed for these records.

In mid-September 2009 when the PO-F and PO-S moorings were deployed, the water column at both sites was stratified, with warm, lower salinity water overlying cooler, saltier water. At both sites, the upper portion of the water column (down to at least 20 m at site PO-F) was fairly well mixed, with clear differences apparent between the deepest instruments (35 m) and the near surface units (Figure 30 and Figure 31). This indicates that the seasonal pycnocline was quite deep at this time. At both moorings, the period of vertical stratification abruptly ends in mid-October when the water column becomes well-mixed (see Figure 32 and Figure 33). This event coincides with the occurrence of a strong northeasterly wind event (Figure XX), which has been shown by Lentz et al. (20??) to be much more effective at achieving vertical mixing than similar strength wind events from other directions. The MD-S and MD-F moorings were deployed in early October 2009 and were located in shallower water than the corresponding PO moorings. The vertical stratification at these moorings is much less intense than at the deeper PO moorings, nonetheless the stratification abruptly disappears at the time of the northeaster.

After the destratratification event in mid-October, the water column continues to cool and remains essentially isothermal until late November. During this period, the deeper moorings (PO-F and PO-S) as well as the MD-S mooring experience moderately large fluctuations (~1 psu) in salinity. The largest signal is observed at the deeper sensors where salinity is observed to increase for several days to a two weeks only to decrease again. The near-surface response is weaker but is generally in the opposite sense; that is a decrease in near-surface salinity occurs at the same time as an increase in deep salinity.

A dramatic hydrographic transistion occurs in late November at all mooring sites. At this time, the deep salinity abruptly increases by approximately 2 psu at PO-S (Figure 31) with lesser increases observed at the other moorings (Figure 30, Figure 34, Figure 35). Contrary to what was

observed in the previous events, in this case, the increase in deep salinity is accompanied by an increase in deep temperature as well. There is also a small decrease in near-surface salinity at this time at all locations except for MD-F. The duration of this event is 3-4 weeks at PO-S and somewhat less at the other locations. At PO-S, there is a brief period, about 2 weeks after the onset of the event, during which time the deep salinity decreases and the near-surface salinity increases. This is quickly followed by the return of the deep saline water. At station PO-S, the peak salinity during this event is nearly 35 psu, whereas the peak at PO-F is approximately 34 psu. This is clearly the same outer shelf/slope water seen during the December 2009 CTD survey.

4.2.2 Winter/Spring 2010 Deployment

UNDER PREPARATION

5 Currents and Sea Level

5.1 Tidal Motions

Characteristics of tidal heights and tidal currents across the OSAMP region were described in some detail using hydrodynamic model output and previously available observations by Codiga and Ullman (2010); the reader is referred to Part 1 for background information on which constituents are most energetic, and the role of surrounding waterbodies such as LIS in shaping the response. This section presents new measurements from moored instrumentation. For the MD-S and MD-F sites (Figure 2), data from October 2010 through June 2010 are used. For the PO-S and PO-F sites the FA09 records are used and not the SP10 records; FA09 records are 4 months long and so better suited for the harmonic analysis than the 3 month SP10 records, which, for tidal quantities, give very similar results in any case. The seven tidal constituents (M2, K1, N2, O1, S2, M4, and L2) that are dominant in the new observations are, as expected, the same as those seen in previous analyses.

Sea level observations were collected only by the PO-S and PO-F moorings. The superposition of the seven main constituents (Figure 42) at these two locations reveals several important features. At both sites there is a distinct spring-neap cycle characterized by neap periods which alternate in their amplitudes, such that every second neap period is typically significantly weaker. During spring conditions, peak-to-peak amplitudes are typically 1.1-1.3 m at PO-S and 1.2-1.4 m at PO-F; during neap conditions they are about 0.5-0.6 m. The daily inequality changes as the spring-neap cycle progresses, and is maximal during spring conditions.

In addition to the minor differences in overall amplitudes between the two sites, small differences in the relative importance of diurnal and semidiurnal constituents, as expected due to their geographic variations (Codiga and Ullman 2010), are apparent.

Tidal current ellipses for each of the seven constituents (Figure 43), based on observed vertical-mean currents, reveal distinct patterns at the MD-S, MD-F, PO-S, and PO-F sites. The relative importance of the constituents, including dominance by M_2, is similar at all four sites. Except for the M_4 constituent at three of the sites, currents rotate clockwise in time. The magnitudes and orientations of the ellipses vary from site to site; for example, M2 ellipses are largest at MD-S, where the major axis is oriented in a NW-SE direction, and at PO-F, where the ellipse is more round. Overall, the geographic variations and many other detailed aspects of the observed current ellipse characteristics from these four sites are in very good agreement with those of the simulation described by Codiga and Ullman (2010).

The vertical variations of tidal ellipse characteristics across the water column, for the dominant M_2 constituent, are clear from plots of the four current ellipse parameters at each of the four sites (Figure 44). In general, as the seafloor is approached amplitudes decay, major axes turn slightly clockwise, and ellipses flatten; the vertical extent off the seafloor in which these changes occur varies from 5-10 m, where currents are most energetic, to less than 5 m. These features are characteristic of theory for frictional tidal boundary layers over a flat seafloor influenced by background rotation (e.g. Soulsby 1990); Codiga and Rear (2004) analyzed ADCP records from the inner shelf south of Block Island Sound, including one record from a site a few km ENE of PO-S where the vertical structure was very similar to that presented here, and demonstrated they compare favorably to the theory. Patterns that diverge from the theory occur in locations influenced by sharp topographic features the bathymetry alters the patterns, which is likely the explanation for why at PO-S, a site where the bottom slopes steeply offshore, the minor axis decreases over most of the water column instead of in a 5-10 m near-bottom layer as the theory would suggest. Owing to the lack of characteristic reversals of velocity in depth, it can be concluded that energetic internal tides are not occurring, unless they are at sufficiently higher frequencies and/or sufficiently intermittent to not be isolated by the harmonic analysis (as seen, for example, by Colosi et al. (2001) on the shelf to the south of Martha's Vineyard).

5.2 Subtidal Motions

TEXT UNDER PREPARATION – Descriptions of Figure 45, Figure 46, Figure 47, Figure 48, Figure 49, Figure 50, Figure 51, Figure 52

5.3 Monthly-Mean Flow and Principal Axes of Weather-Band Currents

TEXT AND FIGURES UNDER PREPARATION

6 Waves

6.1 Wave Parameters from Accelerometers on Multidisciplinary Buoys

TEXT UNDER PREPARATION – Descriptions of Figure 53 and Figure 54

6.2 Directional Wave Parameters from Bottom-Mounted Acoustic Sensors

TEXT UNDER PREPARATION – Descriptions of Figure 53 and Figure 54

6.3 Directional Wave Parameters from Waverider Buoy

TEXT UNDER PREPARATION – Descriptions of Figure 53 and Figure 54

7 Summary

UNDER PREPARATION.

Acknowledgements

Instrument design and preparation by Jim Fontaine was crucial to the success of the vessel-based surveys and PO mooring deployments. We thank Captain Tom Puckett for his superb work on the R/V Cap'n Bert for mooring deployments/recoveries and on the R/V Hope Hudner for the vessel-based surveys, for which Brian Oakley was also very helpful. Candace Oviatt generously provided us with the CTD package for the vessel-based surveys.

References (UNDER PREPARATION)

Codiga, D.L., L.V. Rear. 2004. Observed tidal currents outside Block Island Sound: Offshore decay and effects of estuarine outflow. *J. Geophys. Res.* 109, doi:10.1029/2003JC001804.

Codiga, D.L., D.S. Ullman. 2010. Characterizing the Physical Oceanography of Coastal Waters Off Rhode Island, Part 1: Literature Review, Available Observations, and A Representative Model Simulation. *Prepared for the Rhode Island Ocean Special Area Management Plan 2010*, (Draft March 2010) 2166 pp.

Colosi, J.A., R.C. Beardsley, J.F. Lynch, G. Gawarkiewicz, C.S. Chiu, A. Scotti. 2001. Observations of nonlinear internal waves on the outer New England continental shelf during the summer Shelfbreak Primer study. *J. Geophys. Res.-Oceans* 106, 9587-9601.

Pawlowicz, R., B. Beardsley, S. Lentz. 2002. Classical tidal harmonic analysis including error estimates in MATLAB using T-TIDE. *Computers & Geosciences* 28, 929-937.

Soulsby, R.L. 1990. Tidal-current boundary layers. In: Le Mehaute, B., Hanes, D.M (Ed.), The Sea; Ocean Engineering Science Vol. 9A, Wiley-Interscience, New York, pp. 523-566.

Table 1. Moored instrumentation locations, deployment dates, and sensors.

	MD-S	MD-F	PO-S	PO-F	BIWB
Latitude	41° 06.045'	41° 07.096'	41° 02.869'	41° 14.970'	40° 58.117'
Longitude	71° 34.174'	71° 01.703'	71° 29.972'	71° 05.297'	71° 07.565
Depth [m]	26	34	44.1	43.5	48.2
Dates	Since Oct 9, 2009		FA09: Sep 15, 2009 to Jan 14, 2010 SP10: Mar 19, 2010 to Jun 23, 2010		Since Oct 21, 2009
Sensors: CTD	1, 6, 18m	1, 6, 28m	1, 3, 7, 12, 20, 28, 35m		(none)
Sensors: Currents	Aanderaa 2m; ADCP 5, 6, 7, … 21, 22 m	Aanderaa 2m; ADCP 5, 6, 7, … 30, 31 m	ADCP 4, 5, 6, … 40, 41, 42m	ADCP 4, 5, 6, … 39, 40, 41m	(none)
Sensors: Waves	Accelerometers on discus buoy		Orbital currents from bottom-mounted ADCP		Datawell buoy
Sensors: Meteorology	Winds: 4m Temperature, Pressure: 3m	Winds: 4m Temperature, Pressure: 3m	(none)	(none)	(none)

Notes: See text for abbreviations. The PO-S and PO-F coordinates apply to the bottom-mounted ADCPs; the buoys were within a few hundred meters of them, PO-S buoy at 41° 02.893 71° 30.016 and PO-F buoy at 41° 15.000' 71° 05.500.

Table 2. Vessel-based hydrographic survey dates.

Survey	Dates	Number of Stations
1 – late summer	2009 Sep. 22, 23, 24	45
2 – late autumn	2009 Dec. 7, 8	38
3 – late winter	2010 Mar. 9, 10, 11	45
4 – late spring	2010 Jun. 16, 18	45

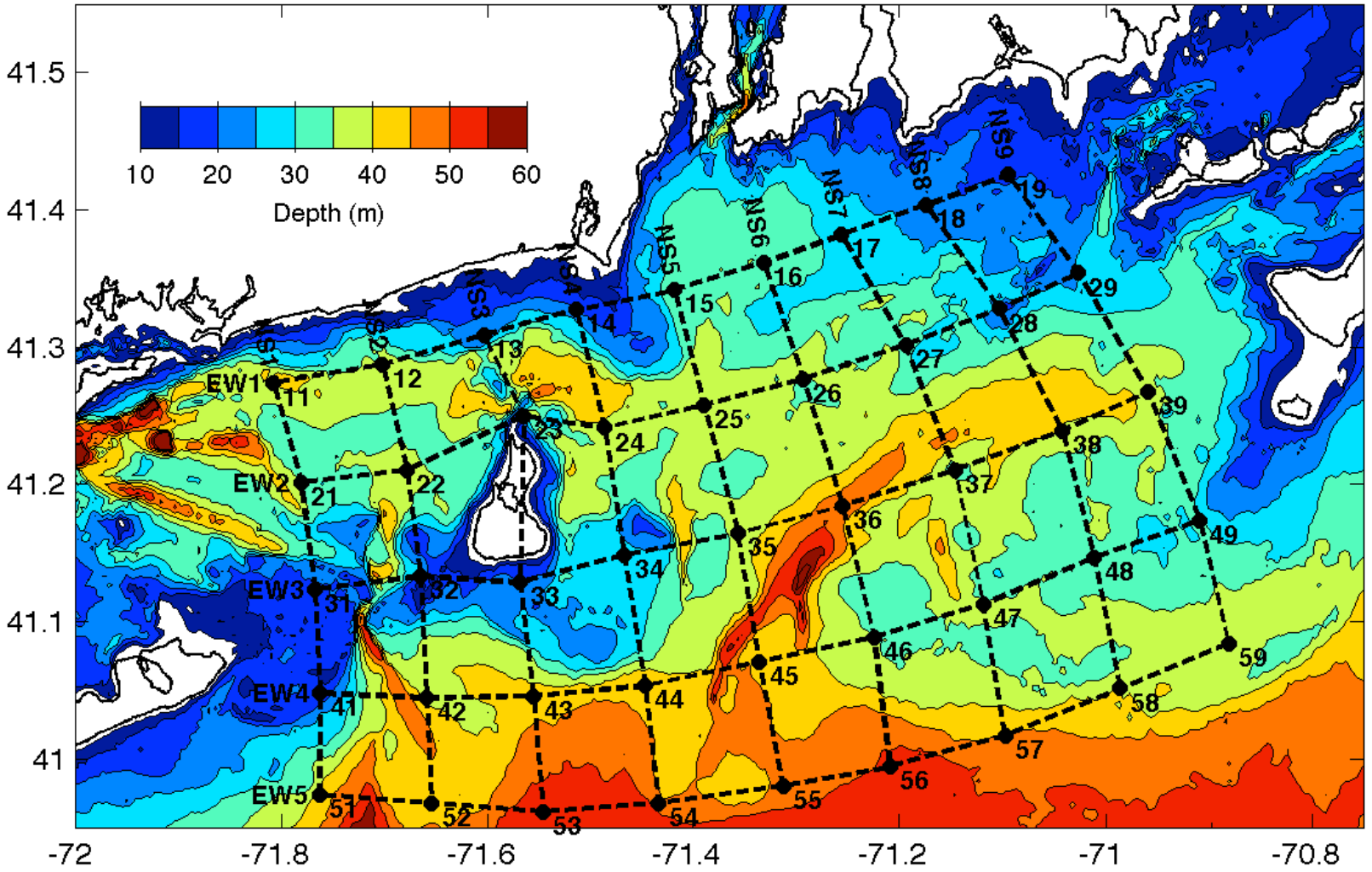

Figure 1. Vessel-based survey station grid superimposed on regional bathymetry.
The dashed lines denote the 9 north-south lines and 5 east-west lines along which vertical sections of hydrographic parameters are presented below.

Figure 2. Moored instrumentation sites: MD-S, MD-F, PO-S, PO-F, and BIWB.

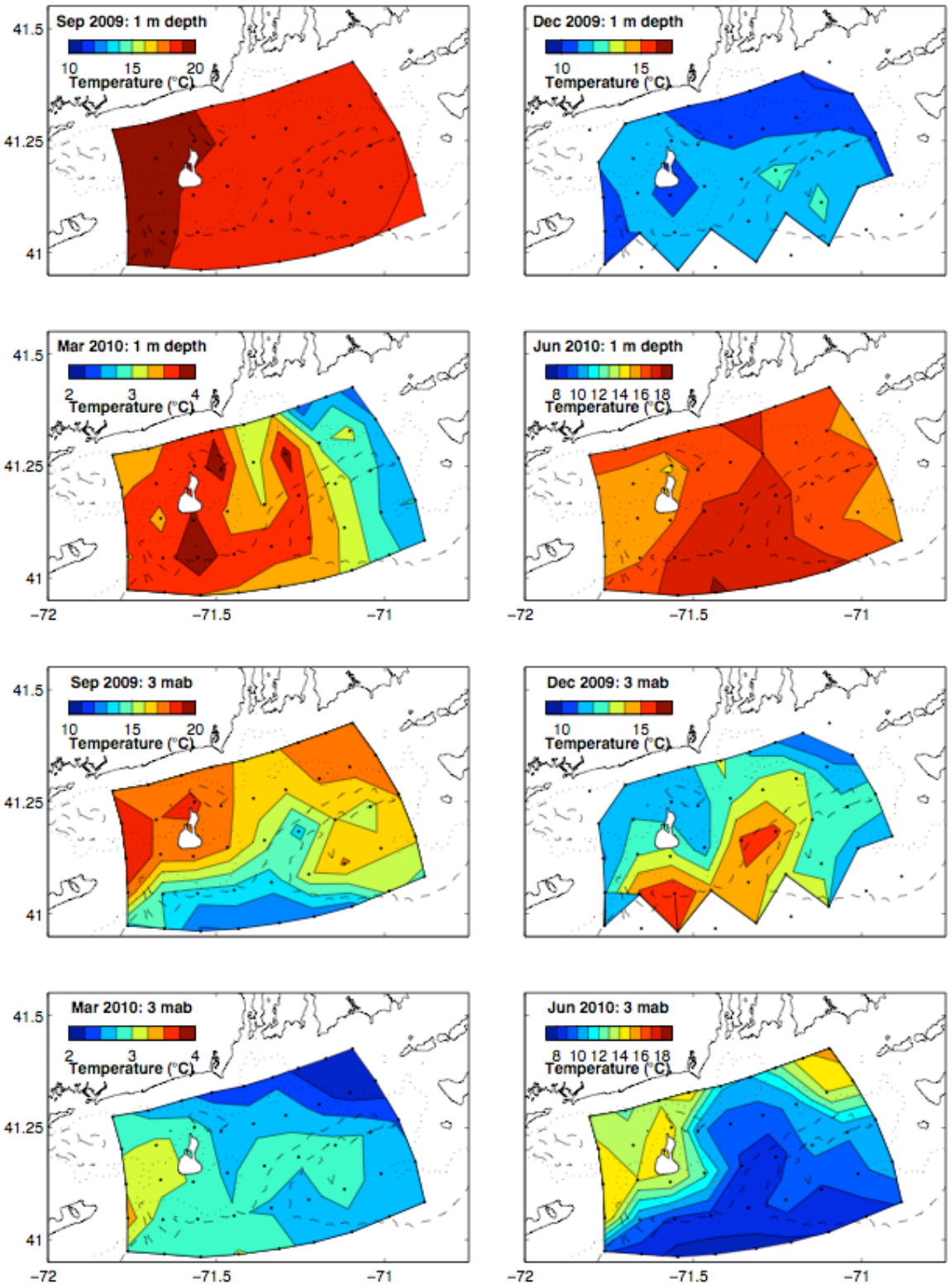

Figure 3. Maps of temperature at 1 m below the surface (top) and 3 m above the bottom (bottom) during all 4 surveys.
The CTD cast locations are denoted by the black dots. The dotted and dashed lines are the 30 m and 40 m isobaths, respectively.